communications physics

A Nature Portfolio journal

Article

https://doi.org/10.1038/s42005-025-02003-6

A snapshot of relativistic motion: visualizing the Terrell-Penrose effect

Dominik Hornof [1,2,7] ✉, Victoria Helm [1,3,4,7], Enar de Dios Rodriguez [5,6], Thomas Juffmann [3,4], Philipp Haslinger [1,2] & Peter Schattschneider[2]

In 1959, Roger Penrose and James Terrell independently predicted that the Lorentz contraction of fast moving objects is not visible in a snapshot photograph. Rather, the object would appear rotated. This surprising effect has never been tested experimentally. Here we demonstrate the Terrell-Penrose effect in a laboratory setting. Using ps-laser pulses and ultra-fast photography with gating times as short as 300 ps, we achieve a virtual reduction of the speed of light to less than 2 m/s, enabling the visualization of relativistically moving objects in real time. Our results comprise simulations and experimentally synthesized snapshots of a sphere and a cube, which are animated to create a slow-motion effect for velocities close to the speed of light. An extension of our method to otherwise unobservable relativistic phenomena, *e. g*. the famous "train" thought experiment revealing the constancy of the speed of light, appears feasible.

In 1924, Anton Lampa published a paper on the visual appearance of a relativistically moving rod in Zeitschrift für Physik[1]. To our knowledge, this is the first discussion of how an observer can effectively measure the relativistic length contraction of a moving rod. Interestingly, the visual appearance of fast-moving 3D objects was not yet an issue at the time. Only in 1959, Roger Penrose[2] (and independently James Terrell[3]) showed that the Lorentz contraction of a moving object is not visible in a snapshot photo. Under quite general conditions, the moving object appears exactly as the object at rest, but rotated. For example, a sphere always appears as a sphere.

The effect is due to the fact that for a photo of a fast-moving object (ideally with exposure time $\to 0$), the light coming from all points of the object must arrive at the same time at the camera. That said, light from more distant points was emitted earlier than light from less distant points. At the earlier time the moving object was at a different position. In the snapshot, the object appears elongated in the direction of movement. This compensates the Lorentz contraction - surprisingly, the compensation is exact and the object appears as if at rest, but rotated around an axis orthogonal to the plane of motion and observation. This assumes that the parallel ray projection is valid (i. e. when the object is much smaller than the distance to the observer). If this is not the case, distortions are induced, as we discuss later in the text. There are a number of excellent simulations, movies and video games dealing with this phenomenon, e.g.[4,5].

On the occasion of the centennial of Anton Lampa's paper we present a genuine lab experiment that visualizes the Terrell-Penrose effect. The idea emerged from our experience with a photographic high speed technique used by the science-art collective SEEC Photography[6], providing real-time information on light reflected from the object[7].

The famous progenitor of high-speed photography is the recording in 1878 of a moving horse[8], rapidly followed by the caption of supersonic motion[9]. Nowadays, CMOS technology allows capturing a finite number of images at GHz rates[10], and gated cameras allow recordings in which moderate imaging rates (kHz) are combined with ultrashort exposures (hundreds of picoseconds). The latter technology is often used in stroboscopic measurements, where fast repetitive phenomena are captured at various delays Δt between the initialization of the process and imaging, thus acquiring a movie of the evolution of the system. In SEEC photography, this is used to visualize the propagation of an ultra-short laser pulse reflected by an *immobile* object: A train of laser pulses is sent toward an object, and the reflected light is captured using a gated camera. The delay Δt between the laser pulses and the exposure is scanned, effectively revealing the motion of pulsed light across the static object. The trick to visualizing relativistic motion is to displace the object by the distance it would move during the delay time Δt.

This way, we simulated a cube moving at 0.8 c (speed of light) and a sphere moving at 0.999 c. In the experiment, the Lorentz contraction must

[1]Vienna Center for Quantum Science and Technology, Atominstitut, TU Wien, Stadionallee 2, Vienna, 1020, Austria. [2]University Service Centre for Transmission Electron Microscopy, TU Wien, Wiedner Hauptstraße 8-10/E057-02, Vienna, 1040, Austria. [3]Vienna Center for Quantum Science and Technology, Faculty of Physics, University of Vienna, Boltzmanngasse 1, Vienna, 1090, Austria. [4]Department of Structural and Computational Biology, Max Perutz Laboratories, University of Vienna, Dr. Bohr Gasse 9, Vienna, 1030, Austria. [5]Kunstuniversität Linz, Hauptplatz 8, Linz, 4010, Austria. [6]IFK, Internationales Forschungszentrum Kulturwissenschaften Kunstuniversität Linz in Wien, Reichsratsstraße 17, Vienna, 1010, Austria. [7]These authors contributed equally: Dominik Hornof, Victoria Helm. ✉e-mail: dominik.hornof@tuwien.ac.at

be applied artificially to mimic relativistic motion, resulting in a cuboid with aspect ratio 0.6 and a sphere essentially squeezed to a disk. Our experimentally synthesized snapshots confirm that the Terrell-Penrose effect balances the Lorentz contraction and leads to the appearance of a rotated noncontracted object.

Methods

Theory

The principle is illustrated in Fig. 1. The definition of a snapshot is that photons reflected (or emitted) from any point on the surface of the object must arrive at the same time at the camera. Let a photon be emitted from point B at t=0 (wiggly line). In order to arrive at the same time at the camera, a photon from point A (closest to the camera) must be emitted when the photon from B passes point A (gray wiggly line), i.e. at a later time $\Delta t = \Delta z/c$. During Δt point A has moved a distance

$$\Delta x = v\Delta t = \beta\, c\, \Delta t = \beta \Delta z \tag{1}$$

to the right to point A', as shown in Fig. 1a. $\beta = v/c$ is the relativistic factor. By symmetry, a photon from point C must be emitted Δt *earlier* than photon B. Thus, the camera takes a snapshot of an elongated object as depicted in Fig. 1b.

Figure 2 shows front views of Fig. 1 (seen from the camera perspective along the z-axis) for different speeds.

Figure 2a, b visualize the Lorentz contracted sphere, which points its north pole towards the camera/observer. Figure 2c and d show the points from which the photons creating the snapshot originated. The sphere appears rotated about the y-axis. One can even look "behind" the equator (green line) and see parts of the southern hemisphere. For a mathematical description of the apparent rotation see supplementary methods 1 and supplementary Fig. 1.

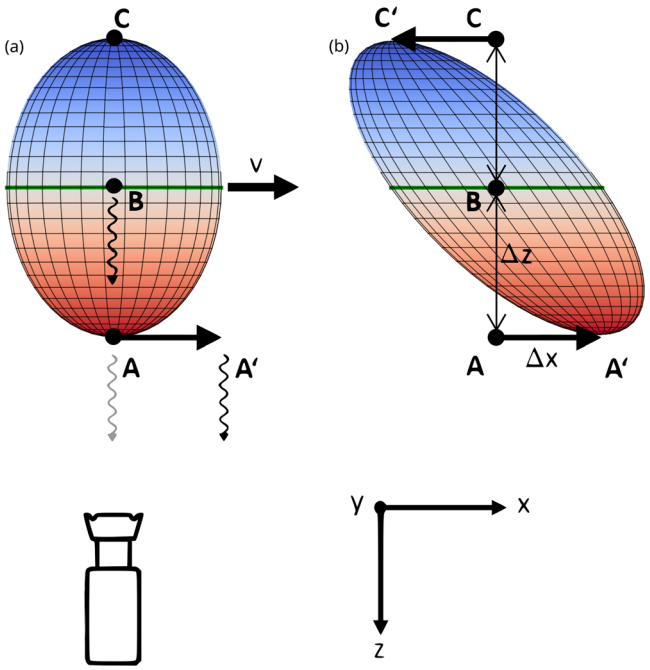

Fig. 1 | Snapshot of relativistic motion. a Top view of a Lorentz contracted sphere moving with speed v = 0.7 c from left to right. In order that photons from A and B arrive at the same time at the camera, photon A must be emitted Δt later when photon B passes A (grey wiggly line). During this time, point A has moved to position A'. By symmetry, a photon from point C must be emitted Δt *earlier* than photon B. **b** In a snapshot, the contracted sphere appears elongated.

Setup

To visualize the Terrell-Penrose effect, we use an ultra-fast photographic technique. We illuminate the object with a pulsed laser and take a photo after a certain delay time. Light reflected from parts of the object that correspond to the respective optical path length will appear bright in this photo. For the sake of clarity we call these photos "slices". Slices taken at a given position of the object are ordered in a temporal sequence. The delay time between two consecutive exposures defines the distance the object would move in the x direction between two exposures. The test object is re-positioned accordingly, and the procedure is repeated. The slices are then combined to frames. They represent experimentally synthesized snapshots, giving a realistic impression of an object moving at relativistic speed.

The setup is sketched in Fig. 3a. A 1035 nm laser from Coherent Corp. produces 1 ps long laser pulses at a 2 MHz repetition rate. The wavelength of light is halved to 517 nm using a BBO crystal. We create a strongly diverging beam using a lens with a focal length of 25 mm. The light scattered off the object is detected by a gated camera (LaVision PicoStar HR12), which is positioned next to the incoming laser beam. The camera and the laser are synchronized using a delay generator.

The camera is able to detect individual photons by using an image intensifier, which is electronically gated to enable ultra-short gating times. The High Rate Image Intensifier (Kentech HRI) consists of three main parts: a photocathode, a microchannel plate (MCP), and a phosphor screen. If the gating is off, the photocathode has a positive potential compared to the MCP. The generated photoelectrons are pushed back to the photocathode. If the gating is on, the polarity of the field is changed. The electrons are pushed to the MCP surface, where they are multiplied depending on the MCP gain settings (MCP voltage). High electric fields accelerate the electrons towards the phosphor screen, which converts them back to photons that are detected by the CCD camera.

Two test objects were chosen: a sphere with a diameter of 1 meter at 0.999 c and a cube with an edge length of 1 meter at 0.8 c (see Fig. 3b, c). Both objects are contracted along the axis of movement by the corresponding Lorentz factor. For this setup, a gating time of 300 ps was used, which

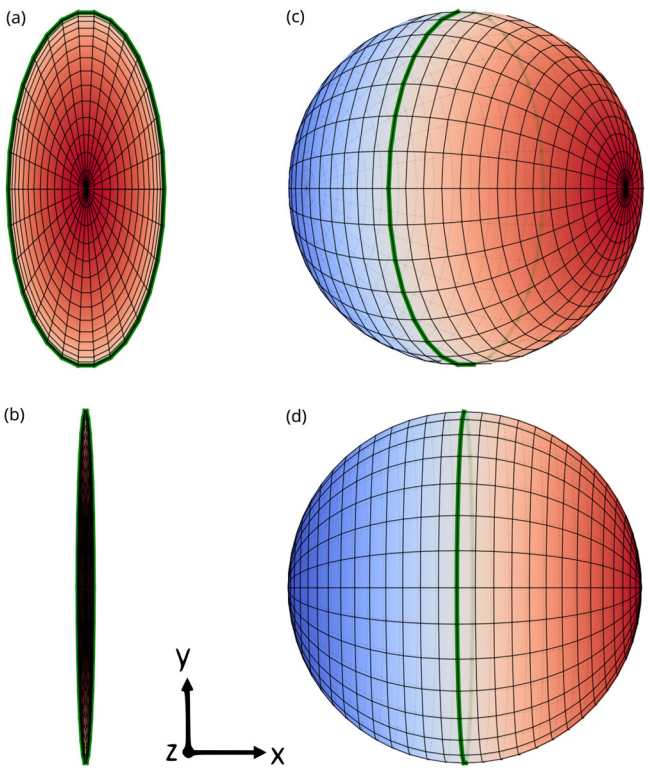

Fig. 2 | Front view of Fig. 1 for two different speeds v = 0.9, and 0.999 c. **a**, **b** Lorentz contracted sphere. The north pole points in direction of the camera. **c**, **d** Terrell-Penrose effect - the sphere appears rotated. The green line indicates the equator.

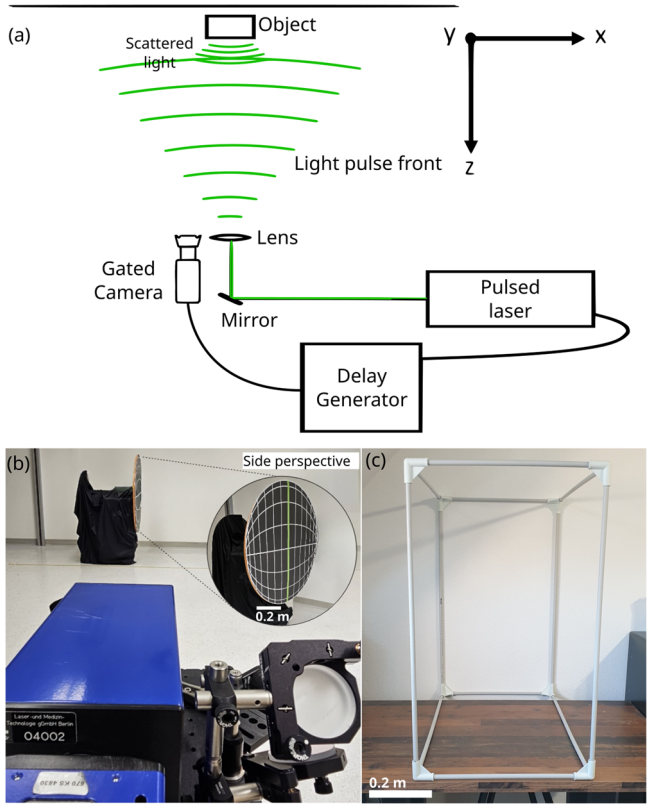

Fig. 3 | Experimental setup. a A pulsed laser beam is focused through a lens to illuminate the entire object. The gated camera is triggered to capture the light scattered back from the object with a certain delay in relation to the laser trigger. **b** The slightly tilted model of the Lorentz contracted sphere seen from the camera (blue) for $v = 0.999\ c$ is almost compressed to a 2D object. The north pole points towards the camera. Next to the camera, the ps-laser pulses are guided via mirrors to a lens in order to expand over the entire field of view. The insert shows the model of the sphere from a different perspective. **c** The Lorentz contracted cube with a side length of $1 \times 1 \times 0.6$ m.

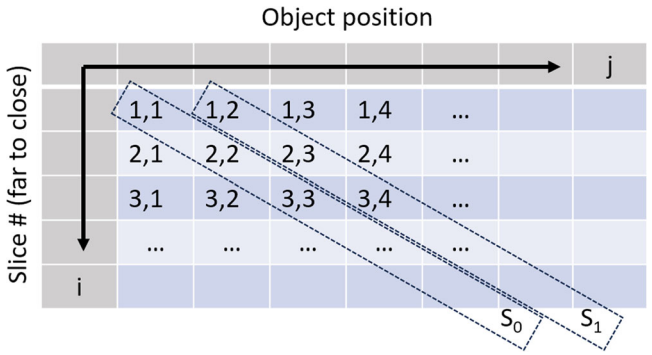

Fig. 4 | Synthesized snapshots. The diagonals S_n represent light that reaches the camera at time $n\,\Delta t$ while the object is moving. $\Delta t = 400$ ps is the time delay between single laser pulses. By combining the series S_n to a movie, we can visualize relativistic motion.

provides both good time resolution and sufficient signal-to-noise. The camera is triggered by the sync output of the laser. For every laser pulse, an electronic signal is generated which is accessible through the sync output. The delay between laser pulses and the camera is varied through a delay generator (Kentech Instruments HDG800).

One image series is generated for each position of the object by taking thirty-two pictures with a time delay between single slices of 400 ps. Light travels 12 cm in that time. This corresponds to $\Delta z = 12$ cm/2 = 6 cm between neighboring slices, since the light first has to travel from the laser to the object, and is then reflected back to the camera. After one image series, the object is displaced in the direction of motion. For any given speed v the necessary displacement Δx between two image series follows from Eq. (1) as $\Delta x = \beta \Delta z$. For the cube moving at 0.8 c this is 48 mm. For the sphere seemingly moving at almost the speed of light, this corresponds to shifting the object by $\Delta x = 6$ cm between two series. Note that in order to simulate Lorentz contraction at 0.999 c, the sphere has to be virtually flat.

With a series of slices $f_{i,j}$, where the indices i and j denote timing and position, respectively, a movie can be created by combining slices to frames S_n of the moving object as

$$S_n = \{f_{i,i+n}, i = 1, N\}. \tag{2}$$

See the sketch in Fig. 4. A single frame contains 17 slices. Acquiring data from 32 positions, we can create an animation with 49 frames (the animations can be seen in the supplementary movies 1&2). The black cover of the supporting structure that serves to move the sphere, see Fig. 3b, is visible in the first 25 frames of the slow-motion clip of the sphere. This results in overexposed regions in the frames, representing an artifact that does not affect our conclusions.

After acquisition of the complete series, the images were post-processed. To reduce noise from each image, we set low signal pixels to 0. As the strength of genuine photonic signals emanating from scattering objects is at least twice that of background noise, this adjustment has no influence on our results, but leads to a significant reduction of background noise.

To create a synthesized snapshot, we sum up the slices to a single frame S_n according to Eq. (2) (Fig. 4). All slices contributing to one frame are normalized to 1, while neglecting hot pixels. This guarantees good visibility of the object, irrespective of its local reflectivity.

Repeating the process for all S_n, an animation of a moving object can be created. In the supplementary slow-motion movies, each sequence of frames is shown at a rate of 30 frames per second. Since light travels a distance of 6 cm between neighboring slices, the apparent speed of light is

$$c \to \frac{0.06\,m}{\frac{1}{30}\,s} = 1.8\,\frac{m}{s}. \tag{3}$$

Results and Discussions

First, one data set of the cube is used for calibration of the system and for analysis of the luminosity distribution as depicted in Fig. 5a. It is not analyzed as described in Fig. 4 using the synthesized snapshots, but rather by taking all the slices of one position and creating an image of the cuboid at rest. It shows the previously described aspect ratio of 0.6, as seen from the camera position (z = 4.2 m, y = -0.12 m). The contour lines are well reproduced, as demonstrated by the superposition with a simulated perspective view (white lines). The aspect ratio agrees with that of the model object in Fig. 3c by 1.5 %. The bottom bars connecting the front and back sides are barely visible because of the shadowing effect from edges and vertices of neighboring slices. The vertices are brighter than the bars due to their higher reflectivity visible in Fig. 3c.

Figure 5b is an experimentally synthesized snapshot of the sphere moving from right to left at 0.999 c. The north pole that pointed towards the camera as shown in Fig. 3b is located at the leftmost rim. The meridians connecting both poles are visible as brighter dots. Closer inspection shows that the horizontal north-south axis is 11% longer than the vertical (equatorial) diameter. This effect is an artifact caused by the necessary tilt of the Lorentz-contracted sphere relative to the light source to ensure proper illumination. The meridians appear discontinuous because they are almost in line of sight seen from the camera.

Figure 5c is a synthesized snapshot of the cube moving from left to right at 0.8 c. As predicted, it appears rotated around the vertical axis. At first sight, the doubling of the front and back faces and the triplicate left upper front

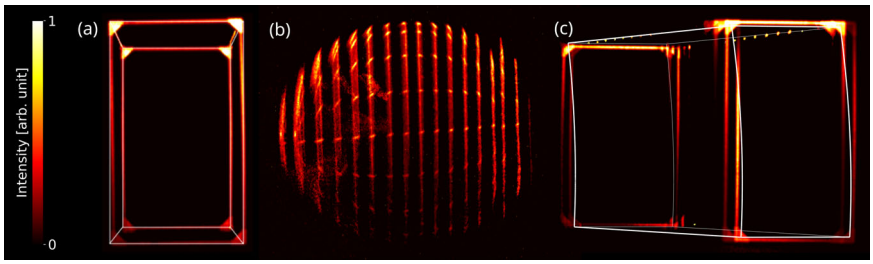

Fig. 5 | Experimental results. a Calibration image of the resting cuboid. The image is superposed with a perspective simulation of a cuboid from the camera position (white lines). **b** Terrell rotation of a deliberately Lorentz contracted sphere moving at 0.999 *c*. **c** Terrell rotation of a cube. A simulation (white contours) is superimposed on the experimental results to guide the view and verify the theoretical description.

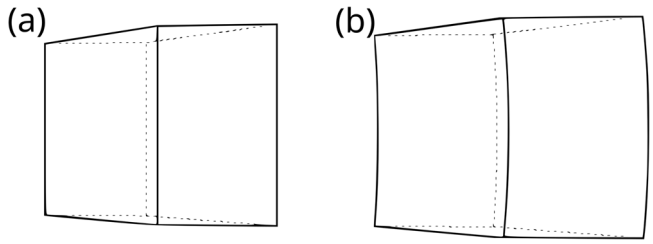

Fig. 6 | Simulation of the cube of 1 m side length moving at 0.8 *c*. a observer at a distance of 100 m (almost parallel illumination). **b** observer at 5 m distance. The distorted vertical edges are hyperbolae.

corner are confusing. Comparison with the simulation (white superimposed contour in Fig. 5c) reveals the cause. The assumption of parallel-ray projection is not strictly valid (see supplementary methods 2). The spherical wave front touches the central parts of the vertical bars earlier, thus moving parts of the front and back faces into neighboring slices. This effect would create the hyperbolae shown in Fig. 6b if the movement were continuous and the gating time infinitely small. The bars connecting the front and back sides appear point-like because—similar to the sphere—they are almost in line of sight. Moreover, the grazing incidence on them back reflects less light into the camera than from the front and back faces. Comparison of the resting with the moving cuboid (Fig. 5a, c) shows that the front sides have the same aspect ratio of 0.6. Only the leading and the trailing sides become elongated by the movement such that the cuboid appears as a rotated cube. An interesting consequence is that although the Lorentz contraction is invisible in a snapshot, it can be measured when the 3-dimensional shape of the object is known as shown for a moving rod by Anton Lampa[1] already in 1924.

Conclusion

This study represents the first experimental visualization of the Terrell-Penrose effect, initially predicted in 1959 based on Anton Lampa's pioneering work published a century ago. Owing to ultrashort gating times down to 0.3 ns[6], a time span in which the pulse moves by less than 10 cm, we were able to demonstrate the invisibility of the Lorentz contraction. Our findings confirm the theoretical models, showing that in a snapshot, objects moving at relativistic speed appear rotated rather than contracted. The detailed visualizations of a sphere and a cube at virtually relativistic speeds align with theoretical expectations, help to understand the elusive Terrell-Penrose effect, and provide intuitive insight into relativistic mechanics. An extension of the method to otherwise unobservable relativistic phenomena, *e.g.* the famous 'train' thought experiment that reveals the constancy of the speed of light, appears feasible.

Data availability

The synthesized snapshots have been generated by data sets acquired with the LaVision PicoStar HR12 camera. Due to the considerable size of these data sets, the corresponding author can provide access to the data upon request.

Code availability

The data files are processed with the Python library *lvpyio* provided by LaVision. The method to create the synthesized snapshots is explained in Fig. 4. The code is available from the corresponding author upon request.

Received: 12 September 2024; Accepted: 11 February 2025;
Published online: 01 May 2025

References

1. Lampa, A. Wie erscheint nach der Relativitätstheorie ein bewegter Stab einem ruhenden Beobachter? *Z. f. Phys.* **27**, 138–148 (1924).
2. Penrose, R. The apparent shape of a relativistically moving sphere. *Math. Proc. Camb. Philos. Soc.* **55**, 137–139 (1959).
3. Terrell, J. Invisibility of the Lorentz contraction. *Phys. Rev.* **116**, 1041–1045 (1959).
4. Kraus, U. First-person visualizations of the special and general theory of relativity. *Eur. J. Phys.* **29**, 1–13 (2008).
5. Sherin, Z. W., Cheu, R., Tan, P. & Kortemeyer, G. Visualizing relativity: The openrelativity project. *Am. J. Phys.* **84**, 369–374 (2016).
6. de Dios Rodríguez, E., Klopfer, B. B., Haslinger, P. & Juffmann, T. SEEC: Photography at the Speed of Light. *Leonardo* **54**, 506–509 (2021).
7. Duguay, M. & Mattick, A. Ultrahigh speed photography of picosecond light pulses and echoes. *Appl. Opt.* **10**, 2162–2170 (1971).
8. Munn, O. & Beach, A. A horse's motion scientifically determined. *Sci. Am.* **39**, 241 (1878).
9. Mach, E. & Salcher, P. Photographische Fixirung der durch Projectile in der Luft eingeleiteten Vorgänge. *Ann. der Phys.* **268**, 277–291 (1887).
10. El-Desouki, M. et al. CMOS image sensors for high speed applications. *Sensors* **9**, 430–444 (2009).

Acknowledgements

We thank Anton Rebhan for valuable comments and Florian Sauer for his support in sample preparation. PH thanks the Austrian Science Fund (FWF) Y1121, P36041, P35953 and the European Capital of Culture Bad Ischl Salzkammergut 2024. TJ acknowledges support from the ERC Micromoupe Grant 758752. PS thanks Arthur C. Clarke and Herbert W. Franke for their inspiring work. This research was funded in whole or in part by the Austrian Science Fund (FWF) [https://doi.org/10.55776/Y1121; https://doi.org/10.55776/P36041; https://doi.org/10.55776/P35953]. For open access purposes, the author has applied a CC BY public copyright license to any author accepted manuscript version arising from this submission.

Author contributions

P.S. proposed the experiment, provided the theoretical part and performed the numerical simulations. D.H., V.H., T.J., P.H. and P.S. designed and built the test objects. V.H., E.d.D.R, T.J. and P.H. performed the experiment and collected the data. D.H. and P.H. conducted the data processing. All authors analyzed and interpreted the results. D.H., V.H. and P.S. produced the figures. D.H., V.H., T.J., P.H. and P.S. wrote the manuscript.

Competing interests

The authors declare no competing interests.

Additional information

Supplementary information The online version contains supplementary material available at https://doi.org/10.1038/s42005-025-02003-6.

Correspondence and requests for materials should be addressed to Dominik Hornof.

Peer review information *Communications Physics* thanks Peng Wang, Jean-Marc Lévy-Leblond and the other, anonymous, reviewer(s) for their contribution to the peer review of this work. [A peer review file is available].